Obtaining three-dimensional models of limb long bones from small mammals: A photogrammetric approach

Ana Filipa Durão[1], Francesc Muñoz-Muñoz[1, *], Jessica Martínez-Vargas[2] and Jacint Ventura[1]

1. Departament de Biologia Animal, de Biologia Vegetal i d'Ecologia, Facultat de Biociències, Universitat Autònoma de Barcelona, Campus de Bellaterra, E-08193 Cerdanyola del Vallès, Spain
2. Chordates Department. Natural Sciences Museum of Barcelona. Parc de la Ciutadella s/n, E-08003 Barcelona (Catalonia, Spain)

* Corresponding author: Francesc Muñoz-Muñoz. e-mail: francesc.munozm@uab.cat

Abstract

The use of two-dimensional (2D) pictures to analyse form variation of three-dimensional (3D) objects entails measurement error, loss of important information and a possible misinterpretation of real shape changes. Despite the increasing availability of 3D imaging technologies, many geometric morphometric analyses of 3D objects are often performed on 2D images for several reasons. This issue is particularly relevant in the study of postcranial bones from small mammals, as devices precise enough for digitising tiny objects are the most expensive ones. In this chapter, we describe a photogrammetric protocol to obtain 3D models of limb long bones from small mammals. The procedure is based on obtaining 2D pictures from different angles using techniques of macro photography. To assess the usefulness of this method for geometric morphometric studies, we compare the form of the humerus between fossorial and semiaquatic water vole species (genus *Arvicola*).

Keywords: *Arvicola*, geometric morphometrics, humerus, macro photography, photogrammetry

1. Background

1.1. 2D *vs* 3D landmark data in form studies

Geometric morphometrics is the statistical analysis of biological form based on two-dimensional (2D) or three-dimensional (3D) Cartesian landmark coordinates (Mitteroecker & Gunz, 2009). In a morphometric context, landmarks are discrete anatomical loci that can be reliably recognised as the same loci in all specimens under study (Zelditch *et al.*, 2004). Although some biological structures are virtually 2D (e.g. insect wings), organisms and their parts are predominantly 3D objects. Therefore, it would seem reasonable that most geometric morphometric studies should use 3D landmarks to assess form variation. In contrast, many 3D biological structures have been studied using 2D images because of the simplicity, efficiency and reduced cost of this technique (Cardini, 2014; Gould, 2014; Muñoz-Muñoz *et al.*, 2016). This practice, however, entails some problems such as measurement error, loss of important information, and a possible misinterpretation of real shape changes (Chiari *et al.*, 2008; Cardini, 2014; Buser *et al.*, 2017). These drawbacks are especially remarkable in structures with an important 3D component (Cardini, 2014). In fact, while a considerable degree of concordance between 2D and 3D datasets has been detected regarding the patterns of size and shape variation of rather flat structures, such as the mandible of the marmot or the mouse, this concordance has been less evident in highly 3D structures, such as the skull of the marmot or the sculpin (Cardini, 2014; Navarro & Maga, 2016; Buser *et al.*, 2017). These results warn about employing 2D landmarks to assess form variation of highly 3D structures, especially at the intraspecific level (Cardini, 2014).

While the use of 2D images to measure morphological variation of 3D biological structures is a widespread practice that will likely contin-

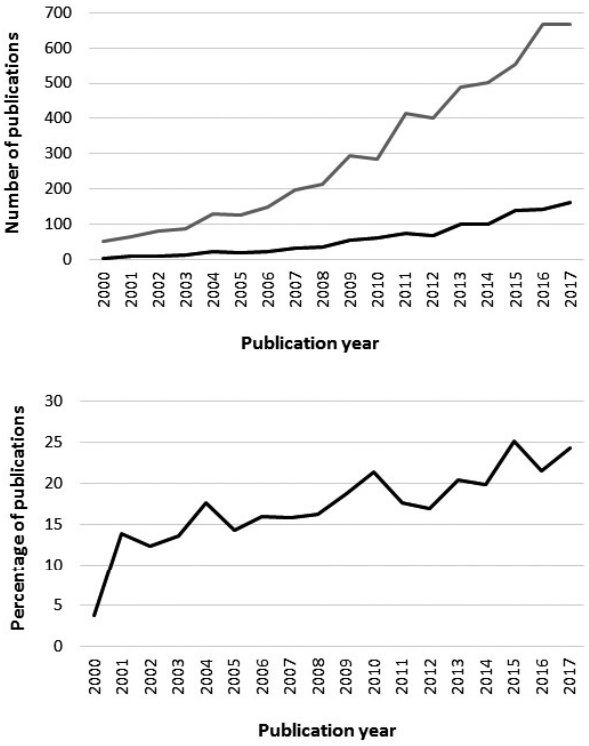

FIGURE **1.** Evolution of the number of 3D geometric morphometric studies from the year 2000 to 2017. The upper panel shows the increase in the total number of geometric morphometric studies (grey line) and in the number of 3D geometric morphometric studies (black line). The lower panel shows the change in the percentage of the latter in relation to the former.

ue for several years (Cardini, 2014), the number of published studies that use 3D landmarks has increased steadily since the development of geometric morphometrics. This trend is illustrated in figure 1, which shows how the number of 3D geometric morphometric studies has evolved between the years 2000 and 2017[1]. The rise of 3D geometric morphometric studies might have several reasons, among which there might be the generalised perception among researchers that using data of the proper dimensionality would improve the results. However, the increasing availability and precision of 3D technologies probably also plays a prominent role in the expansion of this approach. The first 3D geometric morphometric studies almost exclusively obtained landmarks from "big" mammalian skeletal structures, such as the skull of primates or carnivores, with the aid of 3D coordinate digitisers (e.g. O'Higgins & Jones, 1998; Reig *et al.*, 2001). Since then, the technologies to obtain 3D landmarks directly from the object or, alternatively, to obtain 3D models from which landmarks can be recorded, have developed and diversified enormously, and at present allow us to obtain 3D landmarks from a vast array of biological structures.

1.2. THE PARTICULAR CASE OF *SMALL MAMMALS*

Over the last two decades, the use of 3D landmarks has showed an increasing trend, becoming the standard methodology in fields such as anthropology and biomedical research. However, this tendency seems to be somewhat slower in certain groups of animals, as is the case with small mammals[2]. A possible explanation for this fact is that devices precise enough for accurate 3D digitization of tiny objects have a high cost (Muñoz-Muñoz *et al.*, 2016). Nonetheless, this seems to be changing with the increasing variety and accessibility of 3D technologies. Towards the end of the twentieth century, some pioneer studies already employed sets of photographs and statistical methods to obtain 3D landmarks from skulls of small mammals (Fadda *et al.*, 1997; Fadda & Corti, 2001). The methodology followed in these studies involved sets of complex instruments or entailed constraints on the positioning of the objects under study. Maybe for these reasons, this methodology was not generally adopted, and studies of shape variation in small mammals conducted during the following years were mainly based on 2D landmarks

1. The graphs were constructed from the number of publications included in all databases of *Web of Science* containing as a topic "geometric morphometrics" only, and both "geometric morphometrics" and "3D" simultaneously. In order to include the maximum number of published articles on these topics, terminological variants were included in the search with the connector "or": the variants "geometric morphometrics" and "geometric morphometric", and "3D", "three-dimensional", and "three dimensional" were considered. Containing these words as a topic was regarded as indicative of the methodology followed in the article. However, it should be taken into account that a detailed analysis of the literature was not carried out to verify if the articles including these words as a topic actually used these methodologies. Moreover, the search was not exhaustive, and therefore these graphs should be contemplated as approximate.

2. The term *small mammals* does not correspond to any taxonomic category or natural group of mammals. This term is usually used to refer to members of the orders Rodentia, Eulipotyphla and Scandentia, in which the majority of species are small-bodied as compared to most other mammals. Here we use the term *small mammal* to refer to those mammalian species whose skull length is around, or smaller than, 50 millimetres.

recorded on different views of the structure under analysis (e.g. Monteiro *et al.*, 2003; Fernandes *et al.*, 2009; Sans-Fuentes *et al.*, 2009; Kamilari *et al.*, 2013; Wilson, 2013; Yazdi & Adriaens, 2013). More recently, a growing number of studies have employed 3D landmarks to assess form variation of the skull of small mammals (e.g. Evin *et al.*, 2011; Attanasio *et al.*, 2013; Cornette *et al.*, 2013; Martínez-Abadías *et al.*, 2013; Parsons *et al.*, 2014; Gomes-Rodrigues *et al.*, 2016; McIntosh & Cox, 2016a, 2016b; Navarro & Maga, 2016). Because of its complexity and biological importance, the mammalian skull (comprising the cranium and the mandible) is a model structure for the study of morphological variation. Moreover, some species of small mammals, such as the mouse or the rat, are model species in the fields of biomedical research and evolutionary biology. These two factors might explain why analyses of morphological variation of the skull of model species seem to be leading the shift from 2D to 3D. Lately, the form of post-cranial bones, such as limb long bones, of small mammals has also been analysed using 3D data (Caskenette *et al.*, 2016). However, most of the published works analysing the form of post-cranial bones in these animals are still mainly based on 2D pictures (e.g. Echevarría *et al.*, 2014; Marcy *et al.*, 2016; Morgan *et al.*, 2017). Because of the important 3D component of these bones and the difficulty in orienting them in a plane, the use of 3D data to analyse their form seems, at least, appealing. In addition, since the high cost of the devices precise enough for 3D digitization of small objects is a possible cause of the predominance of 2D over 3D studies, the development of more affordable techniques to recover 3D shape of these bones would be of interest.

1.3. Photogrammetry: an affordable and versatile solution

Several technologies to obtain 3D landmarks are currently available, such as coordinate digitisers (e.g. Microscribe™ and Polhemus™), reflex microscopes, automated precision measurement systems (e.g. Micro-Vu Vertex Multisensor Measuring Center™), computed tomography, 3D scanners (including contact scanners, laser scanners, and structured light scanners), and photogrammetry. Of course, each of these techniques has its advantages and drawbacks, and the suitability of each one depends on the particular circumstances, including specific features of the object under study (e.g. the type, its size, its surface), the place where the data or the model will be obtained, or the preferences of the researcher. For example, coordinate digitisers, reflex microscope, and Micro-Vu Vertex allow 3D landmarks to be obtained directly from the object, whereas 3D scanners, computed tomography, and photogrammetry generate 3D digital models or surfaces from which landmarks can be recorded. Having *in silico* models may be interesting when the sample is not easily accessible, as is the case with museum specimens or wild animals, because once you have obtained the model it is always available. This makes it feasible to obtain additional data or revise possible errors without the need to get back to the real specimen. Performing a detailed enumeration and analysis of the pros and cons of each of these technologies is out of the scope of this chapter. However, when the budget is limited, the choice of which technology to use in order to obtain 3D data from tiny objects depends on two main factors, namely the precision of the device and its cost, which tend to be positively associated. Of course, other factors, such as the time needed to obtain the data or the usefulness of the technology in future studies, might also be important when deciding which technology to employ. In this context, we consider photogrammetry a very interesting tool, since it is economical and versatile. Stereophotogrammetry (or photogrammetry for short) estimates 3D coordinates of points on an object using measurements made on two or more 2D images taken from different positions. Thus, the basic equipment needed for photogrammetry consists of a digital camera and specialised software. Because these components have a considerably lower cost than other devices for obtaining 3D data, photogrammetry is usually considered a low-cost method (Chiari *et al.*, 2008; Katz & Friess, 2014; Muñoz-Muñoz *et al.*, 2016). In fact, since some specialised software is freely available on the web and digital cameras are widely accessible, photogrammetry can be performed at virtually no cost. However, obtaining precise models of small objects requires specific photographic material, which increases the overall cost of the technique. Moreover, free software usually offers limited versions of payment software, or only performs some of the utilities of the latter, which at the end implies either using a complex set of specialised programs or buying licensed software. In this study, we used the software PhotoModeler Scanner (Eos System Inc, 2014), which is commercial software with a lifelong license currently listed at $2,995. When com-

pared with that of other technologies, this cost is still limited (Katz & Friess, 2014). However, comparison of costs should be taken with caution since it can change considerably with time. In addition to being cost-effective, photogrammetry has other advantages. One of the most remarkable ones is its versatility. We consider photogrammetry a highly versatile tool for two main reasons. First, photogrammetry allows us to obtain precise 3D models from structures of virtually any size, from earth surface regions (e.g. Haneberg, 2008) to microscopic objects (e.g. Eulitz & Reiss, 2015; Ball *et al.*, 2017). Second, photogrammetry can be performed in a wide range of conditions and places, from the field to the lab or the museum. As a result, we can use photogrammetry to perform studies of very different organisms only adapting the technique to the particular situation by adding or changing some specific devices to the equipment. For example, if we want to obtain the 3D model of a small object (e.g. the skull of a mouse), then a macro lens and a tripod, or another type of camera support, will be indispensable.

Photogrammetry has been widely used in disciplines such as geomorphology, architecture or archaeology. In the field of morphometrics, its possible advantages were already highlighted more than three decades ago (Jacobshagen, 1981). However, studies have only recently started using photogrammetric techniques to recreate 3D models of human (e.g. Katz & Friess, 2014; Hasset & Lewis-Bale, 2017; Quinto-Sánchez *et al.*, 2018) or animal (e.g. Chiari *et al.*, 2008; Falkingham, 2012; Arístide *et al.*, 2013; Evin *et al.*, 2016; Muñoz-Muñoz *et al.*, 2016) phenotypes. Although it is common to combine photogrammetric techniques with macro photography to generate 3D models of small objects in disciplines such as archaeology (e.g. Yanagi & Chikatsu, 2010; Gajski *et al.*, 2016; Marziali & Dionisio, 2017), as far as we know this approach has not been applied to the study of form variation of limb long bones in small mammals. Considering the interest in using 3D data to analyse form variation, and the advantages that photogrammetry offers in recreating small 3D objects, the aim of this study was to establish a protocol that would allow the construction of 3D models of limb long bones from small mammals being appropriate for geometric morphometric analyses. The technical details to obtain the 3D models can be found in the following two sections. In *section 2* we present a list of the equipment employed in this study and their specific utilities in the context of macro photography, whereas in *section 3* we perform a detailed description of the imaging protocol. In order to test the usefulness of the resulting 3D models to analyse form variation, in *section 4* we present a practical case in which we compare the 3D form of the humerus of two different species of the genus *Arvicola*, one fossorial and one semiaquatic, by means of standard geometric morphometric analyses. This case study is performed with a small sample and does not intend to be a detailed analysis of form variation between the two species. It aims to unveil the main size and shape differences of the humerus between the two species and compare the results with previous descriptions.

2. The equipment

2.1. The camera and the lens

When performing photogrammetric 3D reconstructions, the result is entirely dependent on the quality of the photos, so choosing the right camera (or set of cameras) is essential. Almost any camera can be useful to construct 3D models of "big" objects, but when it comes to obtaining precise 3D models of tiny objects it is worth considering to use a digital single-lens reflex (DSLR) camera. The maximum resolution that can be achieved depends, among other things, directly on the number of megapixels the camera has. Professional DSLR cameras give optimal results, but they are very expensive; however, the pictures obtained with mid-priced DSLR cameras yield very good models as well. Although a high resolution is very important, other camera features are to be considered. For example, in macro photography it is crucial to avoid camera vibration during the capture of the picture. Therefore, that a remote trigger can be connected to the camera or, alternatively, that the camera has a delayed-action shutter function, is mandatory (see *section 2.2*). Another interesting camera feature is the possibility to flip and rotate the screen, because it facilitates taking pictures with the camera in any position.

The lens is also an important component of the equipment, especially when we intend to take pictures of small objects. In such a case, the best solution is to use a macro lens. Fixed focal length lenses are preferable for photogrammetry, because they maximise the quality of the photographs and prevent any accidental variable focal lengths, which may occur with a zoom lens. As occurs with the camera, the better the lens, the better the re-

FIGURE 2. Photographic equipment employed to obtain the pictures of the *Arvicola* humeri. The camera with the macro lens, the polarising filter, the tripod, and the remote trigger separately (top) and mounted in front of the humerus fixed to the turntable inside the lightbox (bottom).

sult. Unfortunately, though, also the higher the cost. However, good macro lenses are available at a reasonable cost, being 1:1 macro lenses an interesting option. A magnification ratio of 1:1 means that when the camera is positioned at the closest focus distance, the image formed on the sensor will be the same size as the subject. This magnification is achievable only at the very closest focus distance, which might be a problem in some particular situations (for example, if we want to take photographs of free-moving animals, because they will probably escape).

It is also interesting to add a polarising filter to the lens, because it reduces reflections on shiny surfaces, which is the case with bones. In this study, we used a Canon EOS 750D DSLR camera (24.2 megapixels) equipped with a Tamron 60mm f/2.0 Di II LD macro lens and a polarising filter (figure 2).

2.2. The tripod and the remote trigger

Vibration of the camera during image capture produces blurry photos, especially at low shutter speed. This is a major problem when performing photogrammetric reconstructions because image blur disturbs the visual analysis and interpretation of the data, causes errors, and can degrade the accuracy of automatic photogrammetric processing algorithms. This problem is even greater in macro photography because the depth of field decreases as magnification increases, and a shallow depth of field means that an important part of the picture will be out of focus. A way to increase the depth of field, and therefore the focused portion of the picture, is to set a large F-stop number, which actually means a small aperture of the diaphragm. Under given lighting conditions, taking photographs with large F-stop numbers results in a reduction of the light that arrives at the sensor. Decreasing the shutter speed compensates the loss of light that occurs with small diaphragm apertures, but this increases the problem of camera vibration. In these conditions, the use of a tripod or any other camera support and a remote trigger is essential to obtain focused and sharp images. The self-timer (at a position of 2 seconds), or trigging the shutter by a light touch on the screen in a touchscreen camera, can replace the remote trigger. In this study, we used a Benro Travel Angel FTA 18AB0 aluminium tripod and a Canon RC-6 P/550D remote trigger.

2.3. Lighting

In photogrammetric reconstruction, lighting is important for several reasons. When taking the photos, the light should be intense, diffuse, and uniform. Intense lighting allows to shoot at small diaphragm apertures and at low ISO. Closing the diaphragm increases the depth of field (as explained in *section 2.2*) whereas lowering the ISO reduces the grain and the noise, and both options together result in sharper pictures and better 3D reconstructions. More important than the intensity of light is its evenness. In fact, a soft light with no gleams is preferable to an intense but uneven light (Mallison & Wings, 2014). The uniformity of the lighting will reduce the gleams on shiny objects, and will avoid harsh changes in shadows during the rotation of the subject, which might cause the failure of photogrammetric processing. In order to have good lighting conditions, we used an Amzdeal photo lightbox equipped with a strip of 30 LED lamp beads.

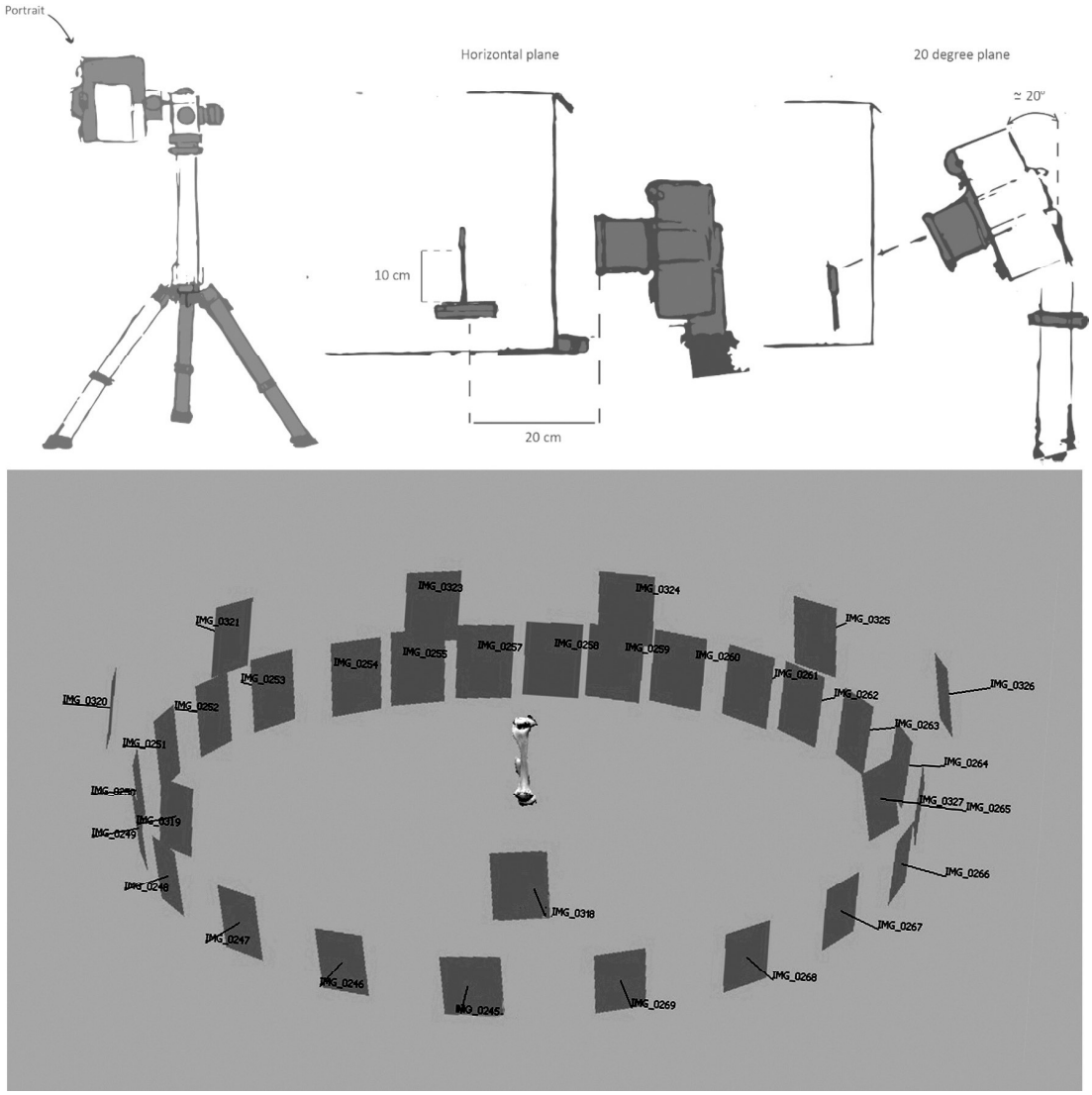

FIGURE **3.** Diagram of the position of the camera during the two complete rotations (top) and picture of the camera positions around the humerus that constitute the imaging protocol (bottom).

2.4. THE "TURNTABLE"

With the aim of obtaining photographs of each humerus from different perspectives, we used the "turntable method", which consists in taking a series of photographs with the camera fixed onto a tripod by rotating the object across a small angle between shots with the aid of a turntable (*section 3*; Mallison & Wings, 2014). Although using an automatic turntable and shooting with the burst mode greatly reduces the time needed to photograph the object, this practice has the inconvenience that some pictures may be poorly focused and that the time intervals between shots could change depending on the speed of the camera. For both reasons, we used a manual rotating device and took the photographs one by one (see *section 3* for details). As a rotating device, we used a Petri dish with the base fixed to the floor of the lightbox and with a printed 360º ruler stuck to the internal face of the lid. As a support to hold the bones, a stick of 10 cm was fixed to the centre of the external face of the lid (figure 2). This stick was used to separate the object from the floor, which makes it easier to take the photographs and crop the bone from the background.

2.5. THE SOFTWARE

Some specialised software is freely available on the web. However, as explained in *section 1.3*, free software usually offers limited versions of payment software or performs very specific functions. Therefore, working with free photogrammetric software finally comes at the price of using a com-

plex set of specialised programs. In this study, we used the commercial software PhotoModeler Scanner (Eos System Inc, 2014).

3. The imaging protocol

As explained in *section 2.4*, images were obtained with the "turntable method" (Mallison & Wings, 2014). Humeri were fixed by their proximal end onto the support with the aid of a reusable putty-like adhesive (Blu Tack™). A tripod was used to fix the camera in a portrait position at a distance of 20 cm from the surface of the lens to the humerus. In order to cover the whole surface of the bone, 33 photographs of each humerus were taken through two complete rotations of 360º with the camera placed at a different height each time (figure 3). In the first whole rotation, the camera (taking the centre of the lens as a reference) was set at the same height as the bone (the horizontal plane). At this height, 24 photographs were taken, by rotating the bone at intervals of 15º. In the second rotation, the camera was set at a height in which the axis of the lens formed an approximate angle of 20º above the horizontal plane. From this angle, nine photographs were taken by rotating the bone at intervals of 40º. Although in principle it is not necessary, the first photograph of each complete rotation was always taken with humeri placed in the same position, i.e. with the caudal surface oriented parallel to the camera lens. The focus was set to manual and adjusted for each shot, in order to get as much focused surface as possible. The camera settings (i.e. the ISO, the F-stop or diaphragm aperture, and the shutter speed) were also adjusted manually to obtain properly exposed pictures. Because we intended to obtain photographs of a small object under controlled conditions of light, the key camera setting was the F-stop. As explained in *section 2.2*, in macro photography large F-stop numbers are desirable to increase the depth of field and consequently the focused part of the subject. However, as the F-stop number increases, so do the diffraction and the blurriness of the image; for this reason, extremely high F-stop numbers were avoided. The general rule of thumb is to use F-stop numbers of about F11 or F16, so we used F16. Because the aperture of the diaphragm was small, a high ISO and/or a low shutter speed were needed to counteract the loss of light. As previously mentioned, the noise increases with the ISO, while a low shutter speed was not a big problem in our case because the camera was fixed onto the tripod and shot with a remote trigger. Therefore, we decided to shoot at ISO 200 and at a shutter speed of 2 seconds to counteract the loss of light.

4. Applying the protocol to the study of the humerus form in fossorial and semiaquatic water voles (genus *Arvicola*)

4.1. Introduction

With the aim of testing the method here described to analyse form variation of skeletal structures in small mammals, we selected a small sample of humeri of two rodent species. Since this bone provides important and rich functional information we compared its form variation in two species that are phylogenetically very close but very different in their ecology and ethology. Specifically, our analyses were focused on two water vole species of the Palaearctic genus *Arvicola*: the southwestern water vole, *Arvicola sapidus*, which occurs in the Iberian Peninsula and much of France (e.g. Ventura, 2007 and references therein), and the montane water vole, *Arvicola scherman* (formerly fossorial form of *Arvicola terrestris*; for details see Musser & Carleton, 2005; but see also Kryštufek *et al.*, 2015), which is found in mountainous areas of southern and central Europe (Musser & Carleton, 2005). While *A. sapidus* is a semiaquatic rodent, *A. scherman* is hypogeal and has a fossorial type of locomotion. Fossorial water voles construct extensive burrow systems in grasslands, pastures, and orchards (Airoldi, 1976). The digging process used by these mammals follows a strict pattern of stereotyped cyclic events; the skull is the main tool for excavation, but the limbs, and particularly the forelimbs, also play an essential role in soil removal (for details see Airoldi *et al.*, 1976). Significant differences between fossorial and semiaquatic water voles in the skeletal structures involved in locomotion, including the humerus, have been described in the literature (e.g. Laville *et al.*, 1989; Laville, 1990; Cubo *et al.*, 2006; Ventura & Casado-Cruz, 2010).

4.2. Data

For analyses, we used the right humerus of ten adult males, five belonging to *A. spidus* and five to *A. scherman*. In each 3D model, 18 landmarks (figure 4; table 1) were collected with the command "Point Auto-detection" of the PhotoMod-

Table 1. Anatomical definitions of the collected landmarks displayed in Figure 4

Landmark	Description
1	Most mid-distal point of the trochlea.
2	Most mid-proximal point of the caudal side of the trochlea.
3	Point of maximum curvature of the olecranon fossa.
4	Most latero-proximal point of the caudal side of the trochlea.
5	Most distal point of contact between the trochlea and the capitulum.
6	Most medial tip of the medial epicondyle.
7	Most lateral point of the lateral epicondylar crest.
8	Point of insertion of the lateral epicondylar crest on the diaphysis.
9	Point of maximum curvature at the distal part of the deltopectoral crest between the deltoid tuberosity and the diaphysis.
10	Most distal point of the deltoid tuberosity.
11	Most proximal point of contact between the deltopectoral crest and the tricipital line.
12	Most distal point of the union between the humerus head and the diaphysis.
13	Most mid-distal point of the great tuberosity at the suture between the proximal epiphysis and the diaphysis.
14	Union between the tricipital line and the greater tuberosity at the suture between the proximal epiphysis and the diaphysis.
15	Most proximal point of the bicipital groove from cranial view.
16	Point of maximum curvature of the suture between the proximal epiphysis and the diaphysis at the groove between the humerus head and the lesser tuberosity.
17	Most mid-proximal point of the cranial side of the trochlea.
18	Most latero-proximal point of the cranial side of the capitulum.

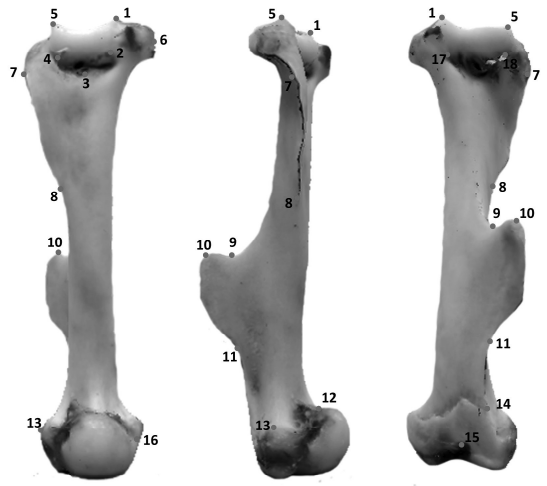

FIGURE **4.** Images of the 3D model of an *Arvicola sapidus* right humerus from caudal (left), lateral (centre), and cranial (right) views indicating the location of the 18 anatomical landmarks (see table 1 for landmark definitions).

eler Scanner software. Morphometric data are affected by measurement error (ME), which is defined as the variability of repeated measurements of a particular character taken on the same individual, relative to its variability among individuals in a particular group (Bailey & Byrnes, 1990). In order to evaluate the ME associated with the landmarking procedure, landmarks were recorded twice by the same person in two separate sessions.

The 3D models were scaled in order to study size. The linear distance between landmark 1 and 15 (ILD 1–15) directly measured on the humerus of each specimen was used to scale the 3D models. Measurements were obtained with a Mitutoy 500-161-21 Digital Caliper (Mitutoyo America Corporation, Aurora, Illinois, USA) with 0.01 mm resolution. To reduce the effect of ME in the scaling of the models, this distance was measured three times in each specimen and the mean of three replicates was used to obtain the scaling factor.

4.3. STATISTICS

Geometric morphometric analyses were performed by implementing the methods included in the MorphoJ software, version 1.06d (Klingenberg, 2011). The form of the humerus was decomposed into size and shape, which were studied separately. Size was estimated through centroid size (CS), which is defined as the square root of the sum of the squared distances from each landmark to the centroid of the configuration (Rohlf & Slice, 1990). Then, the configurations of landmarks were superimposed

Table 2. Results of the nested ANOVA for CS (above) and the Procrustes ANOVA for shape (below)

Effect	SS	% SS	MS	df	F	P
Species	310.388	96.35	310.388	1	216.18	< 0.0001
Individual	11.486	3.57	1.436	8	53.74	< 0.0001
Replicate	0.267	0.08	0.027	10		
Effect	**SS**	**% SS**	**MS**	**df**	**F**	**P**
Species	1.921×10^{-2}	37.07	4.087×10^{-4}	47	5.47	< 0.0001
Individual	2.807×10^{-2}	54.17	7.466×10^{-5}	376	7.73	< 0.0001
Replicate	4.538×10^{-3}	8.76	9.655×10^{-6}	470		

* SS, sum of squares; % SS, percentage of total sum of squares; MS, mean squares; df, degrees of freedom; F, F statistic; P, P-value.

through a generalised Procrustes analysis, and they were projected onto the tangent shape space (Dryden & Mardia, 1998). This procedure removes the variation in the landmark coordinates due to isometric size, position, and orientation, while preserving shape information (Dryden & Mardia, 1998). To assess the effect of ME on size and shape, an analysis of variance (ANOVA) was performed separately for each component of form. To assess the ME in humerus size, a nested ANOVA was conducted with CS as a dependent variable, individual as random factor, replicate as error term, and species as additional main effect (Palmer & Strobeck, 1986). The ME in humerus shape was assessed by means of a Procrustes ANOVA, which is equivalent to the two-factor ANOVA developed by Palmer and Strobeck (1986) but adapted to the study of shape (Klingenberg & McIntyre, 1998; Klingenberg *et al.*, 2002). In this ANOVA, individual was entered as random factor, replicate as error term, species as additional main effect, and the Procrustes coordinates as dependent variables. Although these ANOVAs were originally developed for the study of asymmetry (Klingenberg & McIntyre, 1998; Klingenberg *et al.*, 2002), they can also be used to assess the relative magnitudes of ME from repeated measurements even if structures only from one body side are measured (e.g. Morgan & Álvarez, 2013), as is the case with this study.

Allometry, i.e. size-dependent shape changes, was evaluated with a multivariate regression of shape onto the logarithm of CS (log CS). Statistical significance was calculated using a permutation test with 10,000 iterations under the null hypothesis of no allometric relationship (Monteiro, 1999). In order to visualise the whole set of form changes that allow us to compare our results with those reported in previous studies, and considering that no dependence of shape onto size was detected (see *section 4.4*), subsequent analyses were performed with raw data.

Afterwards, patterns of shape variation were explored with a principal component analysis (PCA) conducted on the variance-covariance matrix of mean individual shapes. A canonical variate analysis (CVA) and a discriminant function analysis (DFA) were conducted to examine the shape features that best distinguished between species. Mahalanobis distance (MD) between species was obtained, together with the statistical significance resulting from permutation test with 10,000 iterations.

4.4. Results and discussion

The ANOVA for CS revealed significant size differences between the humerus of the two species (table 2), with *A. sapidus* having bigger humerus than *A. scherman* (mean CS of 41.4 and 33.5 mm, respectively). These results are completely concordant with those obtained in traditional morphometric studies performed with a sample containing the specimens used in this study (Ventura, 1990, 1992). The ANOVA also revealed that size variation among individuals was significantly larger than variation among replicates (ME), which in fact only represented 0.08% of total CS variation. The Procrustes ANOVA for shape revealed similar results (table 2). Significant differences in humerus shape were also detected between species. As observed for CS, variation among individuals was significantly larger than variation among replicates (ME), although in this case ME represented a higher percentage of shape variation (table 2).

The multivariate regression of shape onto log CS was not significant (9.9%, $p = 0.565$), though this is probably due to the small sample size employed in this study.

The first two PCs resulting from the PCA performed with raw data together explained 63.1% of shape variation. The scatter plot of both PCs showed a non-overlapped arrangement of the two species along PC1, which is consistent with the differences between species detected in the Procrustes ANOVA (figure 5). Shape changes associated

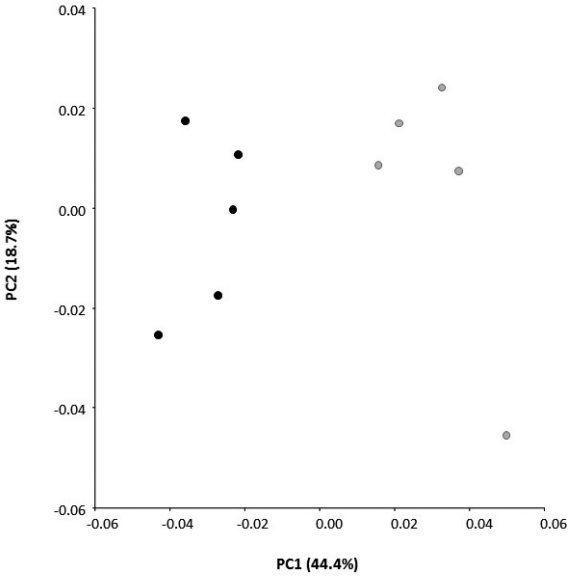

FIGURE 5. Scatter plot of PC1 *vs*. PC2 obtained with raw data. Percentage of shape variation explained by each PC is indicated within parentheses. Black dots belong to Arvicola scherman and grey dots to Arvicola sapidus.

with PC1 indicated that, when compared with *A. sapidus*, the humerus of the fossorial species *A. scherman* shows greater distancing between the zones of muscular insertion and the articular surfaces, which is consistent with previous studies (Laville, 1990). In particular, a relative latero-proximal and caudal displacement of the epycondilar crest, a relative distal displacement and a widening of the deltopectoral crest, and a widening of the proximal and the distal epiphyses were observed when moving from *A. sapidus* to *A. scherman* along PC1 (figure 6). The CVA and DFA analyses confirmed these results, the shape changes between species being almost identical to those associated with PC1. Moreover, despite the small sample size, Mahalanobis' distance between the two species was significant (MD = 3.381, $p = 0.006$).

According to Laville *at al.* (1990), the more distal position of the deltopectoral insertion in relation to the shoulder joint in *A. scherman* increases the efficiency of the acromiodeltoid, spinodeltoid, pectoral and latissimus dorsi muscles. Under a kinematic point of view, this efficiency can be associated with a more active action of pushing and traction of the proximal part of the forelimb during the digging phase in which the humerus is involved. Additionally, shape changes both in proximal and distal epiphyses of the humerus between fossorial and semiaquatic water voles suggest certain interspecific differences in the strength of: i) the scapular muscles involved in the extension, adduction, flexion and rotation of the humerus; ii) the brachialis muscles, and antebrachium flexor; and iii) the elbow ligaments.

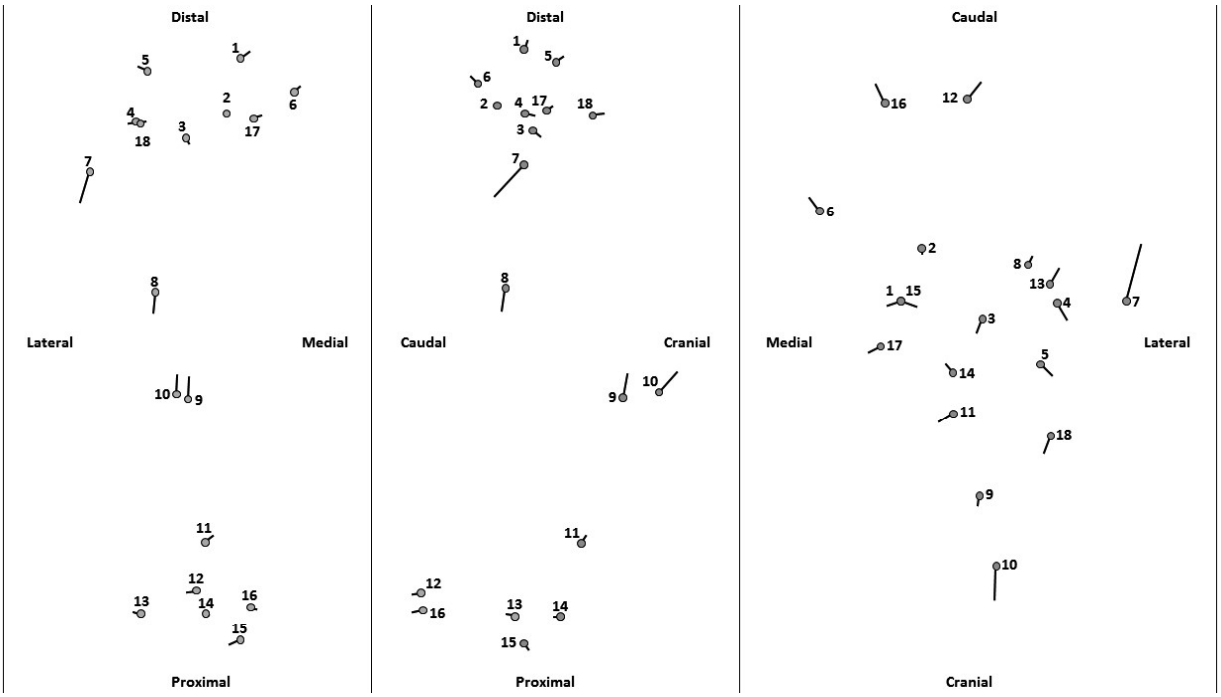

FIGURE 6. Shape changes associated with PC1 from caudal, latero-cranial, and distal views of the humerus (left, centre, and right panels respectively). Grey circles represent the consensus configuration, and vectors represent a shape change of 0.05 units of PC score in the negative direction along the PC axis.

5. Conclusions

In our experience, an important point when performing photogrammetric reconstructions of small biological structures is to establish a specific imaging protocol for the object we intend to model. Since different biological structures differ in their form, colour, and texture, the imaging protocol (including the number and position of the photographs and the camera settings) has to be adapted to these particular traits of the object in order to be useful to obtain the 3D models. However, once the protocol has been established, the 3D models are obtained consistently and with a reasonable time investment.

Previous studies have highlighted that the 3D models obtained with photogrammetry are precise and accurate for morphometric analysis (Muñoz-Muñoz *et al.*, 2016 and references therein). Although we have not specifically tested the accuracy of the method in obtaining 3D models of humeri from small mammals, the changes in size and shape between the two species detected in the case of study are fully consistent with those already described in the literature (Laville *et al.*, 1990). This concordance lets us suggest that the 3D models built with the photogrammetric techniques explained in this chapter are accurate and capture actual morphological differences between the two species. The ANOVAs for size and shape indicated that variation among individuals is significantly larger than variation among replicates, which points out that the technique is precise and that ME error is not an important concern in our study. However, it should to be noted that ME could especially lead to biased results in those studies where interesting variation is subtle, like in fluctuating asymmetry analyses (Palmer & Strobreck, 1986; Klingenberg & McIntyre, 1998; Klingenberg *et al.*, 2002). In fact, the ANOVAs employed in this study have been specifically designed to test if variation in fluctuating asymmetry is larger than ME. Since we have only analysed the right humerus, the magnitude of ME with respect to fluctuating asymmetry, which is usually lower than variation among individuals, remains to be tested. However, the percentage of sum of squares (SS) of the replicate term in our study is similar to the percentages obtained in previous studies, and the total amount of variation of the replicate term is of one order of magnitude lower (see Muñoz-Muñoz *et al.*, 2016 for comparison).

For all these reasons, we conclude that the photogrammetric protocol described in this chapter is a useful and affordable solution to obtain 3D models of limb long bones from small mammals for morphometric analysis.

6. Acknowledgements

This work was supported by Generalitat de Catalunya (grant number 2014-SGR-1241). Ana Filipa Durão received a PIF fellowship from the Universitat Autònoma de Barcelona. The authors acknowledge Anna Chiara Conflitti for her assistance in the capture of the images.

7. References

Airoldi J.P., 1976. Le terrier de la forme fouisseuse du campagnol terrestre, *Arvicola terrestris scherman* Shaw (Mammalia, Rodentia). Zeitschrift für Säugetierkunde 41, 23–42.

Airoldi J.P., Altrocchi, R., Meylan, A., 1976. Le comportement fouisseur du campagnol terrestre, *Arvicola terrestris scherman* Shaw (Mammalia, Rodentia). Revue suisse de Zoologie 83, 282–286.

Arístide, L., Soto, I.M., Mudry, M.D., Nieves, M., 2014. Intra and Interspecific variation in cranial morphology on the southernmost distributed *Cebus* (Platyrrhini, Primates) species. Journal of Mammalian Evolution 21, 349–355.

Attanasio, C., Nord, A.S., Zhu, Y., *et al.*, 2013. Fine tuning of craniofacial morphology by distant-acting enhancers. Science 342(6157).

Bailey, R.C., Byrnes, J., 1990. A new, old method for assessing measurement error in both univariate and multivariate morphometric studies. Systematic Zoology 39, 124–130.

Ball, A.D., Job, P.A., Walker, A.E.L., 2017. SEM-microphotogrammetry, a new take on an old method for generating high-resolution 3D models from SEM images. Journal of Microscopy 267, 214–226.

Buser, T.J., Sidlaukas, B.L., Summers, A.P., 2017. 2D or Not 2D? Testing the utility of 2D vs. 3D landmark data in Geometric Morphometrics of the Sculpin Subfamily Oligocottinae (Pisces; Cottoidea). The Anatomical Record. Electronic publication ahead of print (doi: 10.1002/ar.23752)

Cardini, A., 2014. Missing the third dimension in geometric morphometrics: how to assess if 2D images really are a good proxy for 3D structures? Hystrix, the Italian Journal of Mammalogy 25, 73–81.

CASKENETTE, D., PENUELA, S., LEE, V., BARR, K., BEIER, F., LAIRD, D.W., WILLMORE, K.E., 2016. Global deletion of Panx3 produces multiple phenotypic effects in mouse humeri and femora. Journal of Anatomy 228, 746–756.

CHIARI, Y., WANG, B., RUSHMEIER, H., CACCONE, A., 2008. Using digital images to reconstruct three-dimensional biological forms: a new tool for morphological studies. Biological Journal of the Linnaean Society 95, 425–436.

CORNETTE, R., BAYLAC, M., SOUTER, T., HERREL, A., 2013. Does shape covariation between the skull and the mandible have functional consequences? A 3D approach for a 3D problem. Journal of Anatomy 223, 329–336.

CUBO, J., VENTURA, J., CASINOS, A., 2006. A heterochronic interpretation of the origin of the digging adaptations in the northern water vole, *Arvicola terrestris* (Rodentia, Arvicolidae). Biological Journal of the Linnaean Society 87, 381–391.

DRYDEN, I.L., MARDIA, K.V., 1998. Statistical Shape Analysis. Wiley, Chichester.

ECHEVARRÍA, A.I., BECERRA, F., VASSALLO, A.I., 2014. Postnatal ontogeny of limb proportions and functional indices in the subterranean rodent *Ctenomys talarum* (Rodentia: Ctenomyidae). Journal of Morphology 275, 902–913.

EVIN, A., HORÁČEK, I., HULVA, P., 2011. Phenotypic diversification and island evolution of pipistrelle bats (*Pipistrellus pipistrellus* group) in the Mediterranean region inferred from geometric morphometrics and molecular phylogenetics. Journal of Biogeography 38, 2091–2105.

EVIN, A., SOUTER, T., HULME-BEAMAN, A., AMEEN, C., ALLEN, R., VIACAVA, P., LARSON, G., CUCCHI, T., DOBNEY, K., 2016. The use of close-range photogrammetry in zooarchaeology: creating accurate 3D models of wolf crania to study dog domestication. Journal of Archaeological Science: Reports 9, 87–93

EULITZ, M., REISS, G., 2015. 3D reconstruction of SEM images by use of optical photogrammetry software. Journal of Structural Biology 191, 190–196.

FADDA, C., CORTI, M., 2001. Three-dimensional geometric morphometrics of *Arvicanthis*: implications for systematics and taxonomy. Journal of Zoological Systematics and Evolutionary Research 39, 235–245.

FADDA, C., FAGGIANI, F., CORTI, M., 1997. A portable device for the three dimensional landmark collection of skeletal elements of small mammals. Mammalia 61, 622–627.

FALKINGHAM, P.L., 2012. Acquisition of high resolution three-dimensional models using free, open-source, photogrammetric software. Palaeontologica Electronica 15, 1–15.

FERNANDES, F.A., FORNEL, R., CORDEIRO-ESTRELA, P., FREITAS, T.R.O., 2009. Intra and interspecific skull variation in two sister species of the subterranean rodent genus *Ctenomys* (Rodentia, Ctenomyidae): coupling geometric morphometrics and chromosomal polymorphism. Zoological Journal of the Linnaean Society 155, 220–237.

GAJSKI, D., SOLTER, A., GAŠPAROVIC, M., 2016. Applications of macro photogrammetry in Archaeology. International Archives of the Photogrammetry, Remote Sensing and Spatial Information Sciences 41, 263–266.

GOMES-RODRIGUES, H., ŠUMBERA, R., HAUTIER, L., 2016. Life in burrows channelled the morphological evolution of the skull in rodents: the case of African mole-rats (Bathyergidae, Rodentia). Journal of Mammalian Evolution 23, 175–189.

GOULD, F.D.H., 2014. To 3D or not to 3D, that is the question: do 3D Surface analyses improve the ecomorphological power of the distal femur in placental mammals? PLoS ONE 9, e91719.

HANEBERG, W.C., 2008. Using close range terrestrial digital photogrammetry for 3-D rock slope modeling and discontinuity mapping in the United States. Bulletin of Engineering Geology and the Environment 67, 457–469.

HASSET, B.R., LEWIS-BALE, T., 2017. Comparison of 3D landmark and 3D dense cloud approaches to Hominin mandible morphometrics using structure-from-motion. Archaeometry 59, 191–203.

JACOBSHAGEN, B., 1981. The limits of conventional techniques in anthropometry and the potential of alternative approaches. Journal of Human Evolution 10, 633–637.

KAMILARI, M., TRYFONOPOULOS, G., FRAGUEDAKIS-TSOLIS, S., CHONDROPOULOS, B., 2013. Geometric morphometrics on Greek house mouse populations (*Mus musculus domesticus*) with Robertsonian and all-acrocentric chromosomal arrangements. Mammalian Biology 78, 241–250.

KATZ, D., FRIESS, M., 2014. Technical note: 3D from standard digital photography of human crania: a preliminary assessment. American Journal of Physical Anthropology 154, 152–158.

KLINGENBERG, C.P., 2011. MorphoJ: an integrated software package for geometric morphometrics. Molecular Ecology Resources 11, 353–357.

KLINGENBERG, C.P., MCINTYRE, G.S., 1998. Geometric morphometrics of developmental instability: analyzing patterns of fluctuating asymmetry with Procrustes methods. Evolution 52, 1363–1375.

KLINGENBERG, C.P., BARLUENGA, M., MEYER, A., 2002. Shape analysis of symmetric structures: quantifying variation among individuals and asymmetry. Evolution 56, 1909–1920.

KRYŠTUFEK, B., KOREN, T., ENGELBERG S., HORVÁTH, G.F., PURGER, J.J., ARSLAN, A., CHIȘAMERA, G., MURARIU, D., 2015. Fossorial morphotype does not make a species in water voles. Mammalia 79, 293–303.

LAVILLE, E., 1989. Étude cinématique du fouissage chez *Arvicola terrestris scherman* (Rodentia, Arvicolidae). Mammalia 53, 177–189.

— 1990. Étude morphofonctionelle comparative des structures osseuses impliquées dans le fouissage d'*Arvicola terrestris scherman* (Rodentia, Arvicolidae). Canadian Journal of Zoology 68, 2437–2444.

MALLISON, H., WINGS, O., 2014. Photogrammetry in palaeontology- A practical guide. Journal of Palaeontological Techniques 12, 1–31.

MARCY, A.E., HADLY, E.A., SHERRATT, E., GARLAND, K., WEISBECKER, V. 2016. Getting a head in hard soils: convergent skull evolution and divergent allometric patterns explain shape variation in a highly diverse genus of pocket gophers (*Thomomys*). BMC Evolutionary Biology 16, 207.

MARTÍNEZ-ABADÍAS, N., HOLMES, G., PANKRATZ, T., WANG, Y., ZHOU, X., JABS, E.W., RICHTSMEIER, J.T., 2013. From shape to cells: mouse models reveal mechanisms altering palate development in Apert syndrome. Disease Models and Mechanisms 6, 768–779.

MARZIALI, S., DIONISIO, G., 2017. Photogrammetry and macro photography. The experience of the MUSINT II Project in the 3D digitization of small archaeological artifacts. Studies in Digital Heritage 1, 298–309.

MCINTOSH, A.F., COX, P.G. 2016a. The impact of digging on craniodental morphology and integration. Journal of Evolutionary Biology 29, 2383–2394.

MCINTOSH, A.F., COX, P.G. 2016b. The impact of gape on the performance of the skull in chisel-tooth digging and scratch digging mole-rats (Rodentia: Bathyergidae). Royal Society Open Science 3, 160568.

MITTEROECKER, P., GUNZ, P., 2009. Advances in Geometric Morphometrics. Evolutionary Biology 36, 235–247.

MONTEIRO, L.R., 1999. Multivariate regression models and geometric morphometrics: the search for causal factors in the analysis of shape. Systematic Biology 48, 192–199.

MONTEIRO, L.R., DUARTE, L.C., DOS REIS, S.F., 2003. Environmental correlates of geographical variation in skull and mandible shape of the punare rat *Thrichomys apereoides* (Rodentia: Echimyidae). Journal of Zoology 261, 47–57.

MORGAN, C.C., ÁLVAREZ, A., 2013. The humerus of South American caviomorph rodents: shape, function and size in a phylogenetic context. Journal of Zoology 290, 107–116.

MORGAN, C.C., VERZI, D.H., OLIVARES, A.I., VIEYTES, E.C., 2017. Craniodental and forelimb specializations for digging in the South American subterranean rodent *Ctenomys* (Hystricomorpha, Ctenomyidae). Mammalian Biology 87, 118–124.

MUÑOZ-MUÑOZ, F., QUINTO-SÁNCHEZ, M., GONZÁLEZ-JOSÉ, R., 2016. Photogrammetry: a useful tool for three-dimensional morphometric analysis of small mammals. Journal of Zoological Systematics and Evolutionary Research 54, 318–325.

MUSSER, G.G., CARLETON, M.C., 2005. *Arvicola* Lacépède, 1799; *Arvicola amphibius* (Linnaeus, 1758); *Arvicola scherman* (Shaw, 1801). In WILSON, D.E., REEDER D.M. (eds), Mammal Species of the World. A Taxonomic and Geographic Reference. Third Edition. Johns Hopkins University Press. Baltimore, 963–966.

NAVARRO, N., MAGA, A.M., 2016. Does 3D phenotyping yield substantial insights in the genetics of the mouse mandible shape? Genes, Genome, Genetics 6, 1153–1163.

O'HIGGINS, P., JONES, N., 1998. Facial growth in *Cercocebus torquatus*: an application of three-dimensional geometric morphometric techniques to the study of morphological variation. Journal of Anatomy 193, 251–272.

PALMER, A.R., STROBECK, C., 1986. Fluctuating asymmetry: measurement, analysis, patterns. Annual Reviews in Ecology, Evolution and Systematics 17, 391–421.

QUINTO-SÁNCHEZ, M., MUÑOZ-MUÑOZ, F., GOMEZ-VALDES, J., *et al.*, 2018. Developmental pathways inferred from modularity, morphological integration and fluctuating asymmetry patterns in the human face. Scientific Reports 8, 963.

REIG, S., DANIELS, M.J., MACDONALD, D.W., 2001. Craniometric differentiation within wild-living cats in Scotland using 3D morphometrics. Journal of Zoology 253, 121–132.

ROHLF, F.J., SLICE, D., 1990. Extensions of the Procrustes method for the optimal superimposition of landmarks. Systematic Zoology 39, 40–52.

SANS-FUENTES, M.A., VENTURA, J., LÓPEZ-FUSTER, M.J., CORTI, M., 2009. Morphological variation in house mice from the Robertsonian polymorphism area of Barcelona. Biological Journal of the Linnaean Society 97, 555–570.

VENTURA, J., 1990. Datos biométricos sobre los huesos largos y la escápula de *Arvicola sapidus* Miller, 1908 (Rodentia, Arvicolidae). Boletín de la Real Sociedad Española de Historia Natural (Sección Biología) 86, 55–64.

— 1992. Morphometric data on the scapula and limb long bones of *Arvicola terrestris* (Linnaeus, 1758) (Rodentia, Arvicolidae). Revue suisse de zoologie 99, 629–636.

— 2007. *Arvicola sapidus* Miller, 1908. In Palomo, L.J., Gisbert, J. (eds.): *Atlas de los Mamíferos terrestres de España*. DGCNA-MIMAM, SECEM, SECEMU. Madrid, 362–365.

VENTURA, J., CASADO-CRUZ, M., 2011. Post-weaning ontogeny of the mandible of fossorial water voles: ecological and evolutionary implications. Acta Zoologica 19, 12–20.

WILSON, L.A.B., 2013. Geographic variation in the greater Japanese shrewmole, *Urotrichus talpoides*: combining morphological and chromosomal patterns. Mammalian Biology 78, 267–275.

YANAGI, H., CHIKATSU, H., 2010. 3D Modelling of small objects using macro lens in digital very close range photogrammetry. International Archives of Photogrammetry, Remote Sensing and Spatial Information Sciences 38, 617–622.

YAZDI, F.T., ADRIAENS, D., 2013. Cranial variation in *Meriones tristrami* (Rodentia: Muridae: Gerbillinae) and its morphological comparison with *Meriones persicus*, *Meriones vinogradovi* and *Meriones libycus*: a geometric morphometric study. Journal of Zoological Systematics and Evolutionary Research 51, 239–251.

ZELDITCH, M.L., SWIDERSKI, D.L., SHEETS, H.D., FINK, W.L., 2004. Geometric Morphometrics for Biologists. A Primer. Elsevier Academic Press, San Diego.